A new two-way nesting technique based on the smoothed semi-prognostic method

Jinyu Sheng, Richard J. Greatbatch, Xiaoming Zhai, and Liqun Tang

Department of Oceanography, Dalhousie University, Halifax, NS, Canada, B3H 4J1

Keywords:
Two-way nesting, semi-prognostic method, ocean model, shelf circulation, Scotian Shelf, Meso-American Barrier Reef System.

Short title: A NEW TWO-WAY NESTING TECHNIQUE

SUBMITTED TO *OCEAN DYNAMICS*

Abstract.

A new two-way nesting technique is presented for a multiple nested-grid ocean modelling system. The new technique uses the smoothed semi-prognostic (SSP) method to exchange information between the different subcomponents of the nested-grid system. Four versions of the new nesting technique are described, together with conventional one-way nesting. The performance of the different nesting techniques is compared, using two independent nested-grid modelling systems, one for the Scotian Shelf of the northwest Atlantic Ocean and the other for the Meso-American Barrier Reef System of the northwestern Caribbean Sea. Nesting using the semi-prognostic method is shown to effectively prevent unrealistic drift of the inner model, while use of the SSP method avoids unnecessary damping of small scales on the inner model grid. Comparison of the annual-mean flow field with the near-surface currents determined by Fratantoni (2001) from observed trajectories of near-surface drifters demonstrates the overall superiority of the two-way nesting technique based on the SSP method.

1. Introduction

Ocean circulation models have increasingly been used to simulate circulation and temperature/salinity (T/S) distributions in the ocean. Physical processes affecting the ocean circulation operate over a wide range of temporal and spatial scales. To fully resolve all these different scales using a numerical model with a uniform grid is a formidable task. Usually one is faced with a choice between a basin-scale simulation at a relatively coarse resolution to resolve mainly the large-scale circulation features, or a regional-scale simulation with a very high resolution to resolve small-scale features such as fronts and eddies within a limited area domain. In a limited-area simulation, a prior knowledge is required to describe physical processes at work along model open boundaries, and interaction between the basin-scale, used to prescribe the boundary conditions, and the smaller-scale circulation within the model domain are prohibited. Sometimes a large-scale model contains choke points (such as the Gulf Stream separation region) where a very high-resolution simulation would be an advantage, although such high resolution is not required over the rest of the domain. In such circumstances, a nested-grid modelling system may be advantageous, in which a finer-resolution inner model is embedded inside a coarser-resolution outer model. Indeed, the main advantage of a nested-grid modelling system is to increase the model resolution in subregions to resolve fine-scale circulation features without having the computational expense of using high-resolution over the whole model domain (Fox and Maskell 1995).

In the past, two basic approaches have been used to exchange information between the subcomponents of a nested-grid modelling system. The first is conventional one-way (C1W) nesting in which a fine-resolution inner model is connected to a coarser-resolution outer model only through the specification of the open boundary conditions for the inner model, these being taken from the outer model-computed fields. The main advantage of C1W nesting is that the outer and inner models can be run sequentially and it is therefore computationally efficient. There are two main disadvantages. First, there is no constraint from the outer model on the interior of the inner model domain. This can lead to drift of the inner model and result in a flow field in the inner model that differs radically from that in the outer model (the two examples given in this paper illustrate

this effect). Second, C1W nesting does not allow feedback from the inner model to the outer model with the result that the outer model does not benefit from the finer resolution within the inner model domain.

The second approach to nesting allows for two-way interaction between the subcomponents of a nested modelling system, in addition to the specification of open boundary conditions for the inner model based on the outer model fields. Two-way interaction can be achieved in many ways. A commonly used technique is to transfer information between the two grids at a narrow zone (or dynamic interface) near the grid interface (Kurihara et al. 1979; Ginis et al. 1998). The coarse-grid model variables, such as currents, T/S and associated fluxes at the dynamic interface are interpolated onto the fine grid to provide time-dependent boundary conditions for the fine grid, and the fine-grid model variables are interpolated back onto the coarse grid to update the coincident coarse-grid values at the dynamic interface. It should be noted that the dynamic interface of this nesting scheme can be considered as an internal boundary for the coarse-grid model, and the coarse-grid integration is not necessary over the subregion covered by the fine-grid domain. Clearly, a possible disadvantage of this method is that, as in C1W nesting, the outer model does not constrain the interior of the inner model domain directly, and, hence, there is nothing to prevent unrealistic drift of the inner model.

An alternative two-way nesting technique, suggested by Oey and Chen (1992), is to embed a fine-resolution inner model inside a coarser-resolution outer model and use the inner model variables to replace the outer model variables over the subregion where the two grids overlap. This two-way nesting technique has the advantage of allowing a two-way interaction at the grid interface, and also allows the outer model to benefit directly from the finer resolution of the inner model where the two grids overlap. Nevertheless, there is still no direct constraint on the evolution of the inner model within the interior of its domain.

The new technique to be presented here is similar to Oey and Chen (1992) in that a fine-grid inner model is embedded inside a coarser-grid outer model. Different from Oey and Chen's nesting approach, we use the smoothed semi-prognostic (SSP) method (Eden

et al. 2004; Greatbatch et al. 2004) to exchange information between the interiors of inner and outer models where their domains overlap. An advantage of semi-prognostic nesting is that the inner and outer models are always coupled throughout their region of overlap, so that drift of the inner model, independent of the outer model, is effectively eliminated. It should be noted that the new nesting technique can easily be applied to a multiply nested-grid modelling system with one or more fine-resolution inner models embedded inside a coarser-grid outer model, and one or more finer-resolution local submodels embedded inside each inner model, and so on.

The arrangement of this paper is as follows. Section 2 describes the new two-way nesting technique based on the SSP method. Sections 3 and 4 discuss the performance of the new nesting technique using two independent nested-grid modelling systems, one for the Scotian Shelf of the northwest Atlantic Ocean and the other for the Meso-American Barrier Reef System of the northwestern Caribbean Sea. The final section gives a summary and conclusions.

2. A new two-way nesting technique based on the smoothed semi-prognostic method

The unique feature of the new two-way nesting technique is the use of the smoothed semi-prognostic (SSP) method (Eden et al. 2004; Greatbatch et al. 2004) to exchange information between the subcomponents of a nested-gridded modelling system. The SSP method is a modification of the original semi-prognostic method (OSP) (as introduced by Sheng et al. (2001)), to eliminate damping on small scales (e.g. the mesoscale). The original application of both the OPS and SSP methods was to provide a simple way to adjust a model for systematic error (see Greatbatch et al. (2004) for a comprehensive overview). Indeed, the semi-prognostic method is closely related to the "pressure-correction method" described by Bell et al. (2004), and which is also a technique to correct for systematic bias in a model. In the semi-prognostic method, the adjustment is accomplished by replacing the density variable ρ in the model's hydrostatic equation by a linear combination of the model-computed density ρ_m and an

input density ρ_c:

$$\rho = \alpha\rho_m + (1-\alpha)\rho_c \tag{1}$$

where α is the linear combination coefficient with a value between 0 and 1. In Sheng et al. (2001), the input density ρ_c is computed from a monthly mean climatology of hydrographic data, but it might also be density from another model, as in the nesting technique to be described here.

Equation (1) can be rewritten as:

$$\frac{\partial p}{\partial z} = -g\rho_m - g(1-\alpha)(\rho_c - \rho_m) \tag{2}$$

where the second term on the right hand side of the above equation is the correction term used to correct for model systematic error and unresolved processes. Eq. (2) is the form of the original semi-prognostic (OSP) method introduced by Sheng et al. (2001). As stated in Sheng et al. (2001), the above procedure is equivalent to adding a forcing term to the horizontal momentum equations (see also Greatbatch et al. 2004). This can be demonstrated by decomposing the model pressure p into two terms:

$$p = p^* + \hat{p} \tag{3}$$

where p^* is the traditional pressure variable satisfying

$$\frac{\partial p^*}{\partial z} = -g\rho_m \tag{4}$$

with $p^* = g\rho_0\eta$ at the sea surface, and $\hat{p}$ is a correction term satisfying

$$\frac{\partial \hat{p}}{\partial z} = -g(1-\alpha)(\rho_c - \rho_m) \tag{5}$$

with $\hat{p} = 0$ at the sea surface. Using (3), the horizontal momentum equations can be rewritten as:

$$\frac{\partial \vec{u}}{\partial t} = -\frac{1}{\rho_o}\nabla_h p^* - \frac{1}{\rho_o}\nabla_h \hat{p} + \ldots \tag{6}$$

where $\vec{u}$ is the horizontal velocity vector and ∇_h is the horizontal Laplacian operator. Therefore, the semi-prognostic method is equivalent to adding a body forcing term $(-\frac{1}{\rho_o}\nabla_h\hat{p})$ to the model horizontal momentum equations. It is important to note that

the semi-prognostic method is adiabatic, leaving the temperature and salinity equations unadjusted (Greatbatch et al. 2004). Therefore, the semi-prognostic method makes no compromise to the requirement that the flow be primarily in the neutral tangent plane in the ocean interior, and the method is well-suited for use in tracer studies (e.g. Zhao et al. 2004).

The OSP method, however, has the drawback that its damps the mesoscale eddy field. Eden et al. (2004) introduced the smoothed semi-prognostic (SSP) method by applying the correction term only on large spatial scales:

$$\frac{\partial p}{\partial z} = -g\rho_m - g(1-\alpha) < \rho_c - \rho_m > \tag{7}$$

where <> represents the spatial averaging. Eden et al. (2004) demonstrated that the SSP method is effective at eliminating the damping effect of the OSP method on the mesoscale eddy field.

If the input density ρ_c in (2) is the density from another model, the semi-prognostic method becomes a technique for transferring information into and between models (effectively "assimilating" data from one model to the other). As such, the semi-prognostic method can be used to construct a two-way interactive nesting technique for a nested-grid ocean circulation modelling system to be described as follows.

For convenience of the presentation in this paper, we consider a simple nested-grid modelling system in which a high-resolution inner model is embedded inside a coarser-resolution outer model. In addition to the use of the outer model-computed fields to specify open boundary conditions for the inner model, the new two-way nesting technique (referred to as the SSP nesting technique) consists of the following two steps. First, the outer model density ρ_{outer} in the overlapping subregion is used to adjust the inner model based on

$$\frac{\partial p_{inner}}{\partial z} = -g\rho_{inner} - g(1-\beta_i) < \hat{\rho}_{outer} - \rho_{inner} > \quad \text{(for the inner model)} \tag{8}$$

where p_{inner} is the pressure variable of the inner model, ρ_{inner} is the inner model density, $\hat{\rho}_{outer}$ is density calculated from the outer model T/S fields after interpolation onto the inner model grid, β_i is a linear combination coefficient with a value between 0 and 1,

and <> is the smoothing operator. The use of the smoothing operator ensures that the inner model is constrained by the outer model only on large scales (determined by the smoothing scale that is used), the smaller scales associated with the fine grid of the inner model being free to evolve without constraint.

Second, the inner model density in the overlapping subregion is used to adjust the outer model in the same overlapping subregion based on

$$\frac{\partial p_{outer}}{\partial z} = -g\rho_{outer} - g(1-\beta_o) < \hat{\rho}_{inner} - \rho_{outer} > \qquad \text{(for the outer model)} \qquad (9)$$

where p_{outer} is the pressure variable of the outer model, ρ_{outer} is the outer model density, $\hat{\rho}_{inner}$ is density calculated from the inner model T/S fields after interpolation onto the outer model grid, β_o is a linear combination coefficient with a value between 0 and 1, and <> is a smoothing operator, which is usually different from that in (8). Indeed, the smoothing operator in (9) can be chosen so that the correction term applies only on small scales (rather than only on large scales, as in (8)), in which case, the operator <> in (9) is really the inverse of a smoothing operator. For the present application, the second smoothing operator is not used.

It can be seen from (8) and (9) that the new two-way nesting technique based on the SSP method is easy and straightforward to implement since only the hydrostatic equations of the subcomponents of the nested-grid modelling system have to be modified. Physically, as shown in (6), the SSP nesting technique is equivalent to adding an interaction term $(-\frac{1}{\rho_o}\nabla_h\hat{p})$ to the inner and outer model momentum equations, respectively. The interaction term depends on the density difference between the inner and outer models, with the linear coefficients β_i and β_o in (8) and (9) determining the intensity of the interaction. In the case of $\beta_o = 1$, the outer model in the overlapping subregion is not constrained by the inner model. In the case of $\beta_i = 1$, the inner model is not constrained by the outer model except for specification of the inner model boundary conditions based on the outer model results. As a result, the conventional one-way (C1W) nesting technique mentioned in the introduction is equivalent to setting $\beta_o = \beta_i = 1$ in (8) and (9).

For simplicity, we refer to the SSP nesting technique with $\beta_i = \beta_o = 0.5$ as the

SSP two-way (SSP2W) nesting technique, and the one with $\beta_i = 0.5$, and $\beta_o = 1$ as the SSP one-way (SSP1W) nesting technique (Table 1). If the unsmoothed correction terms (i.e., the OSP method) are used in (8) and (9), the nesting technique is referred to as the original semi-prognostic (OSP) nesting technique. We refer to the OSP nesting technique with $\beta_i = \beta_o = 0.5$ as the OSP two-way (OSP2W) nesting technique, and the one with $\beta_i = 0.5$ and $\beta_o = 1$ as the OSP one-way (OSP1W) nesting technique (Table 1). It can be seen that the main difference between the SSP1W (OSP1W) case and the C1W case is that that hydrostatic equation over the interior of the inner model domain in the SSP1W (OSP1W) case is constrained directly by the outer model density through the SSP(OSP) method, which is not true in the C1W case. (The OSP nesting technique was originally introduced in Sheng and Tang (2004); this method, however, leads to damping on the scale of the fine grid, and for this reason the SSP method described here is to be preferred - see Section 4.)

It should be noted that the four variants of the new nesting technique discussed above (i.e., SSP2W, SSP1W, OSP2W and OSP1W cases, see Table 1) rely only on the exchange of the model density fields in the hydrostatic equations of the inner and outer models. As noted earlier, this is equivalent to modifying the momentum balance in the models. In particular, the model currents, temperature and salinity fields are not exchanged directly between the two models, except for the use of the outer model results to specify the open boundary conditions for the inner model. Furthermore, the temperature and salinity equations for the component models are unchanged by the nesting procedure. It follows that both the SSP and OSP nesting techniques are adiabatic. Adiabaticity ensures that the new nesting technique based on the semi-prognostic method does not compromise the requirement for the flow in the ocean interior to be primarily in the neutral tangent plane (Greatbatch et al. 2004), and also ensures that the new nesting technique based on the smoothed semi-prognostic method is well-suited for tracer studies (Zhao et al. 2004).

The new two-way nesting technique can also be combined with the original version of the SSP method described in Eden et al. (2004); that is to correct for model systematic error and unsolved processes in multi-year simulations. Taking the inner

model as an example, the hydrostatic equation of the inner model can be rewritten as

$$\frac{\partial p_{inner}}{\partial z} = -g\rho_{inner} - g(1-\beta_i) < \tilde{\rho}_i - \rho_{inner} > \tag{10}$$

with the input density $\tilde{\rho}_i$ defined as

$$\tilde{\rho}_i = \alpha_i \hat{\rho}_{outer} + (1-\alpha_i)\rho_c \equiv \hat{\rho}_{outer} + (1-\alpha_i)(\rho_c - \hat{\rho}_{outer}) \tag{11}$$

where ρ_c is the climatological density calculated from climatological T/S fields, and α_i is the linear coefficient between 0 and 1. In the case of $\alpha_i = 0$, the input density $\tilde{\rho}_i$ is determined solely by the climatological density (ρ_c). In the case of $\alpha_i = 1$, $\tilde{\rho}_i$ is determined solely by the density calculated from outer model T/S fields after interpolation onto the fine grid ($\hat{\rho}_{outer}$), and climatological density does not affect the hydrostatic equation of the inner model.

Similarly, the hydrostatic equation of the outer model can be rewritten as

$$\frac{\partial p_{outer}}{\partial z} = -g\rho_{outer} - g(1-\beta_o) < \tilde{\rho}_o - \rho_{outer} > \tag{12}$$

with the input density $\tilde{\rho}_o$ defined as

$$\tilde{\rho}_o = \alpha_o \hat{\rho}_{inner} + (1-\alpha_o)\rho_c \equiv \hat{\rho}_{inner} + (1-\alpha_o)(\rho_c - \hat{\rho}_{inner}) \tag{13}$$

where ρ_c is the climatological density, as before, and α_o is a linear coefficient between 0 and 1. In the case of $\alpha_o = 0$, the input density $\tilde{\rho}_o$ is determined solely by the climatological density (ρ_c). In the case of $\alpha_i = o$, $\tilde{\rho}_o$ is determined solely by the density calculated from inner model T/S fields after interpolation onto the coarse grid ($\hat{\rho}_{inner}$), and climatological density does not affect the hydrostatic equation of the outer model.

In the application to the Scotian shelf described in Section 3, $\alpha_i = 1$ (that is, there is no correction made to the inner model using climatological data), but $\alpha_o = 0.5$ (i.e., climatological data is used to correct the outer model). For the application to the Meso-America Barrier Reef system described in Section 6, both α_i and α_o are set to 0.5. Outside the common subdomain of the inner and outer models, climatological data is used to adjust the outer model in both cases with $\alpha_o = 0$ and $\beta_o = 0.5$. It should be noted that, for both the nested systems, the original semi-prognostic method is used in the outer model outside the overlapping subregion.

Finally we note that the nested-grid modelling systems described in sections 3 and 4 use the subgrid-scale mixing parameterization scheme of Smagorinsky (1963) for the horizontal eddy viscosity and diffusivity with the Prandtl number set to 0.1. Since the Smagorinsky scheme is resolution dependent, it has the desirable effect of leading to different levels of mixing in the inner and outer models. The vertical mixing scheme is the same in both the inner and outer models and uses Csanady's (1982) formula in the surface mixed layer and Large et al.'s (1994) formula in the interior of the ocean, with the Prandtl number set to 1.

3. Nested-grid modelling system of the Scotian Shelf

We first assess the performance of the new nesting technique using the nested-grid modelling system developed by Zhai et al. (2004) for the Scotian Shelf (SS) of the northwest Atlantic Ocean based on the primitive-equation, z-level ocean circulation model known as CANDIE (Sheng et al. 1998). The reader is referred to Sheng et al. (2001) and Zhai et al. (2004) for a detailed description of the model parameters and model setup. In this paper, we provide only a brief summary of the key elements of the system. We note that there is demand for high resolution information on currents and temperature and salinity variations on the Scotian Shelf because of the growing offshore oil and gas industry, as well as aquaculture activities nearer shore, and it is for this reason that a nested modelling system for the region is of interest. An application of the nested modelling system to simulate the response of the Scotian Shelf to Hurricane Juan in 2003 can be found in Sheng et al. (2004).

The nested system for the Scotian Shelf comprises a fine-grid inner model and a coarse-grid outer model (Fig. 1). The fine-resolution inner model covers the area between 54°W and 66°W and between 39°N and 47°N, with a horizontal resolution of one eleventh degree in longitude (about 7 km). The coarse-resolution outer model is the northwest Atlantic Ocean model developed by Sheng et al. (2001), which covers the area between 30°W and 76°W and between 35°N and 66°N, with a horizontal resolution of one third degree in longitude. Both the inner and outer models use the ETOPO5 bathymetry (a gridded elevation/bathymetry compiled by the U.S. National Geophysical

Data Center, National Oceanic and Atmospheric Administration) and have 31 unevenly spaced z levels, with the centers of each level located at 5, 16, 29, 44, 61, 80, 102, 128, 157, 191, 229, 273, 324, 383, 450, 527, 615, 717, 833, 967, 1121, 1297, 1500, 1733, 2000, 2307, 2659, 3063, 3528, 4061, and 4673 m, respectively.

The model boundary conditions of the nested system are specified as follows. At the closed lateral boundaries of the inner and outer models, the normal flow, tangential stress of the currents and horizontal fluxes of T/S are set to zero (free-slip conditions). Along the model open boundaries, the normal flow and T/S fields are specified using the adaptive open boundary condition (Marchesiello et al. 2001), which first uses an explicit Orlanski radiation condition (Orlanski 1976) to determine whether the open boundary is passive (outward propagation) or active (inward propagation). If the open boundary is passive, the model prognostic variables are radiated outward to allow any perturbation generated inside the model domain to propagate outward through the open boundary as freely as possible. If the open boundary is active, the model prognostic variables at the open boundary are restored to input boundary fields. For the inner model, the input boundary fields are the simulated currents and T/S fields produced by the outer model after interpolation onto the fine grid, with a restoring time scale of 1 day. For the outer model, the input boundary fields are the monthly varying climatologies of T/S from Geshelin et al. (1999), the depth-mean normal flow is taken from the diagnostic calculation of Greatbatch et al. (1991), and the restoring time scale is 15 days.

The nested system of the Scotian Shelf is initialized with the January mean temperature and salinity and forced by the monthly mean COADS (Comprehensive Ocean-Atmosphere Data Set) wind stress and surface heat flux, the latter using the method of Barnier et al. (1995). The model sea surface salinity is restored to the monthly varying climatology with a time scale of 15 days. We conduct five numerical experiments by integrating the nested system for two years with the same model forcing and same sub-grid scale mixing parameterizations but using the five different nesting techniques listed in Table 1. Since the nested system is driven by monthly mean forcings, the interaction rate between the inner and outer models is set to be once per day in this study. For the results shown here, the correction term in (8) is smoothed over 16 inner

model grid points; that is, 112 km.

We first examine the simulated circulation and temperature over the northwest Atlantic Ocean produced by the outer model using the SSP2W nesting technique (the SSP2W case). The upper ocean circulation at day 690 (i.e., December 1 of the second model year, assuming 360 days for a model year) is shown in Fig. 2. In agreement with observations (Lazier and Wright 1993; Loder et al. 1998), there is a narrow southeastward jet along the shelf breaks of the Labrador and Newfoundland Shelves (the offshore branch of the Labrador Current). On reaching the northern flank of the Grand Banks, the offshore branch of the Labrador Current splits into three parts: a coastal branch that flows through the Avalon Channel, a middle branch that flows through Flemish Pass to the south, and an eastern branch that passes around the seaward flank of Flemish Cap. The middle branch and part of the eastern branch merge over the eastern flank of the Grand Banks and form a narrow equatorward jet along the shelf breaks of the Grand Banks and the Scotian Shelf. The outer model also produces reasonably well the general flow patterns of the Gulf Stream and North Atlantic Current offshore from the continental slopes of the Grand Banks and the Scotian Shelf. The large-scale circulation features produced by the outer model in the other four cases (i.e., the SSP1W, OSP2W, OSP1W and C1W cases), as well as the single-domain model results presented in Sheng et al. (2001), are essentially the same as shown in Fig. 2. The main difference is that the outer model results using the two-way nesting technique (i.e., the SSP2W and OSP2W cases) have more meso-scale features over the SS and adjacent slope and a slightly stronger recirculation over the slope water region due to the feedback from the inner model to the outer model in the SSP2W and OSP2W cases.

We next examine the detailed circulation and temperature over the Scotian Shelf and slope where the inner and outer model grids overlaps. The sub-surface (61 m) circulation at day 690 over this region produced by the inner model in the SSP2W case (Fig. 3b) is characterized by two southwestward jets on the Scotian Shelf, with an inshore jet (the Scotian Current) flowing along the coast and an offshore jet (the shelf-break jet) flowing along the outer shelf. Over the slope water region off the SS, there are two meso-scale recirculation gyres and an intense eastward flow as part of

the Gulf Stream (Fig. 3b). This eastward jet splits into two branches at about 62°W, with the main branch flowing southeastward into the deep water and the weak branch flowing northeastward between the main branch and the shelf-break jet. The sub-surface temperature at day 690 produced by the inner model in the SSP2W case is characterized by cold intermediate waters of less than 5°C over the most of the Scotian Shelf, warm waters of greater than 20°C over the deep water, and sharp temperature gradients in the slope water region (Fig. 3b). The SSP2W nested inner model also reproduces a cold water tongue associated with the Labrador Current at the shelf break of the SS, which is one of the most important circulation features over the SS and slope water region associated with the spreading of the Labrador Current from the Grand Banks to the Scotian Shelf (Smith et al. 1978; Loder et al. 1998).

The large-scale circulation features produced by the outer model in the SSP2W case (Fig. 3a) and those produced by the inner model in the SSP1W, OSP2W and OSP1W cases (Fig. 3c-e) compare reasonably well to those produced by the inner model in the SSP2W case (Fig. 3b). Main differences occur in the meso-scale features over the slope water region. The inner model in the SSP2W case generates more meso-scale features over the SS and slope, and a better defined cold water tongue at the shelf break of the SS than the outer model (Fig. 3a,b), which is expected since the inner model has a three times finer horizontal resolution than the outer model. In comparison with the inner model results in the SSP2W and SSP1W cases, the inner model results in the OSP2W and OSP1W cases have less meso-scale circulation features in the slope water region, which is due mainly to the damping effect of the original semi-prognostic method on the meso-scale eddy field discussed in section 2.

Figure 3f shows the inner model results in the C1W case, in which the inner model is connected to the outer model only through the specification of the inner model boundary conditions taken from the outer model. As a result, the inner model can drift away from the outer model, as is evident in Figure 3f. The inner model in the C1W case fails to generate the Scotian Current near the coast and the shelf-break jet associated with the Labrador Current at the shelf break of the SS. The C1W nested inner model also fails to produce the widely recognized recirculation in the slope water region and

overestimates significantly the sub-surface slope water temperature. Instead, the C1W nested inner model generates unrealistically large and broad northeastward flow over the slope water region, which differs significantly from the inner model results in other four cases (Figures 3b-e). The failure of the C1W case highlights one of the advantages of semi-prognostic nesting; namely, to prevent unrealistic drift of the inner model.

The second year model results in the five cases are used to calculate the annual mean near-surface currents over the SS and slope region at 16 m depth (Fig. 4). Figure 4b, for the inner model in the SSP2W case, shows the annual mean southwestward Scotian Current, the narrow shelf break jet, and the narrow jet over the slope water offshore from the SS that first flows northeastward over the slope water region off the southwestern SS and then turns eastward to the deep water off the southeastern SS. Further south of the slope water region, there is a strong and broad eastward flow as part of the Gulf Stream. The annual mean circulation produced by the SSP2W nested inner model is consistent with our current knowledge of time-mean circulation in the SS and slope (Lazier and Wright 1993; Loder et al. 1998; Smith et al. 1978; Sheng and Thompson 1996). The annual mean near-surface currents produced by the inner model in the SSP1W, OSP2W and OSP1W cases (Fig. 4c-e) compare reasonably well with the annual mean near-surface currents produced by the SSP2W nested inner model results (Fig. 4b). By contrast, the annual mean near-surface currents produced by the inner model using the C1W nesting technique (Fig. 4f) differ significantly from the inner model results in the other four cases shown in Fig. 4b-e.

To further demonstrate the advantage of the new two-way nesting technique based on the smoothed semi-prognostic method, we compare the annual mean near-surface (15 m) currents produced by the nested system with the time mean currents in the 1990s inferred by Fratantoni (2001) from the observed trajectories of near-surface drifters over the SS and slope. The annual mean currents produced the inner model in the SSP2W and SSP1W cases (Fig. 4b,c) reproduce reasonably well the large-scale features of the observed currents. The SSP2W outer model results (Fig. 4a) are also in qualitative agreement with the observed currents. To quantify the misfit between the observed and

model-calculated near-surface currents, we use a value of γ^2 defined as

$$\gamma^2 = \frac{\sum_k{}^N[(u_k{}^o - u_k{}^s)^2 + (v_k{}^o - v_k{}^s)^2]}{\sum_k{}^N[(u_k{}^o)^2 + (v_k{}^o)^2]} \tag{14}$$

where $(u_k{}^o, v_k{}^o)$ are the horizontal components of the observed near-surface currents at the kth location estimated by Fratantoni (2001), $(u_k{}^s, v_k{}^s)$ are the horizontal components of the simulated near-surface currents at the same location as the observations, and N is the total number of locations where observed estimates are available. Clearly, the smaller γ^2, the better the model results fit the observations.

For the nested-grid system of the SS using the SSP2W nesting technique, the γ^2 value is about 0.73 for the outer model and 0.61 for the inner model (Fig. 5a,b and Table 1), indicating that the inner model performs better than the outer model in reproducing Fratantoni's observed currents. The inner model in the OSP2W and OSP1W cases also reproduces reasonably well the time-mean observed near-surface currents over the SS and slope (Fig. 4d,e and 5d,e), with γ^2 values of about 0.65 in both cases (Table 1), which are comparable to, and slightly larger than, the γ-values in the SSP2W and SSP1W cases, indicating that the nested-grid system of the SS using the original semi-prognostic (OSP) nesting technique performs slightly worse than that using the smoothed semi-prognostic (SSP) nesting technique in reproducing Fratantoni's data. The inner model results in the C1W case agree the least well with Fratantoni's time-mean observed near-surface currents (Fig. 5f), with the γ^2 value of about 1.01, which is about 60% larger than that of the inner model results in other four cases (Table 1).

4. Nested-grid modelling system of the Meso-American Barrier Reef System

We next assess the performance of the four variants of the new nesting technique using the nested-grid modelling system developed by Sheng and Tang (2004) for the Meso-American Barrier Reef System (MBRS) over the northwestern Caribbean Sea. The reader is referred to Sheng and Tang (2004) for a detailed description of the model parameters and setup of the system. Only a brief summary of the system is provided

here. We note that there is an increasing demand for a nested modelling system for the MBRS since this area serves as an important breeding and feeding ground for marine mammals, reptiles, fish and invertebrates, many of which are of commercial importance. The MBRS also contributes significantly to the protection of coastal landscapes and the maintenance of coastal water quality. The unique marine ecosystems in the MBRS have been significantly affected by natural and anthropogenic influences such as eutrophication of coastal waters, excessive terrestrial runoff and sedimentation from deforestation. Reliable simulations of the ocean circulation in the MBRS using a nested-grid model are required for an effective management of the coastal and marine ecosystems in the area.

The nested system for the MBRS comprises the fine-grid inner model and the coarse-grid outer model shown in Fig. 6. The inner model domain covers the area between 79°W and 89°W and between 15.5°N and 21.5°N, with a horizontal resolution of about 6 km. The outer model is the western Caribbean Sea model (Sheng and Tang 2003), which covers the area between 72°W and 90°W and between 8°N and 24°N, with a horizontal resolution of about 19 km. The nested-grid system of the MBRS uses the same vertical discretization with 31 z-levels, the same sub-grid mixing parameterizations and the same formulation for the open boundary conditions as the nested system of the Scotian Shelf, except that the depth-mean flow along the outer model open boundaries of the MBRS nested system is the depth-mean flow taken from a (1/3)° FLAME model simulation of the North Atlantic Ocean (FLAME stands for the Family of Linked Atlantic Model Experiments, Dengg et al. 1999). The nested system of the MBRS is initialized with January mean climatologies of temperature and salinity and forced by the monthly mean COADS wind stress and surface heat flux, with the model sea surface salinity restored to the monthly mean climatology, as before. Also, as before, the inner and outer models interact once per day, and the smoothing scale in (8) corresponds to 16 model inner model grid points (that is about 112 km). Similarly, we conduct five numerical experiments by integrating the nested system of the MBRS for two years using the five different nesting techniques listed in Table 1.

The sub-surface (61 m) circulation at day 720 (end of December of the second

model year) produced by the SSP2W nested outer model is dominated by the Caribbean Current flowing from the northern Colombian Basin to the western Yucatan Basin, with two cyclonic recirculations in the southwestern Caribbean Sea known as the Panama-Colombia Gyre (Fig. 7). The Caribbean Current is relatively broad and almost westward in the central and eastern Colombian Basin. This current bifurcates before reaching Nicaragua Rise, with one small branch veering southwestward to form the Panama-Colombia Gyre. The main branch of the current turns northwestward and flows onto the northwest Caribbean Sea to form an offshore flow running westward off the northern coast of Honduras. This offshore flow turns northward as it approaches the Gulf of Honduras and then runs northward along the east coast of Belize and Mexico. The simulated sub-surface temperature at day 690 produced by the SSP2W outer model (Fig. 7) is characterized by a strip of warm sub-surface water of about 27°C along the pathway of the Caribbean Current over the northern Colombian Basin and southwestern Cayman Basin, with two pools of cold waters associated with the cyclonic Panama-Colombia Gyre over the southwestern Colombian Basin. The SSP2W nested outer model results are essentially same as the single-domain model results of the western Caribbean Sea discussed in Sheng and Tang (2003) and in general agreement with our current knowledge of general circulation in the region (Mooers and Maul 1998; Johns et al. 2002).

The outer model results in the other four cases (i.e., SSP1W, OSP2W, OSP1W, and C1W) have very similar large-scale features as those produced by the outer model in the SSP2W case. The main differences occur in the meso-scale features over the northwestern Caribbean Sea. The outer model in the SSP2W and OPS2W cases produces more meso-scale features over this region than those in the SSP1W, OSP1W and C1W cases, which is due to the feedback from the inner model to the outer model.

Figure 8 shows the detailed sub-surface (61 m) currents and temperature at day 720 produced by the nested system in the five cases over the northwestern Caribbean where the outer and inner model grids overlap. The sub-surface circulation at this time produced by the SSP2W nested inner model (Fig. 8b) is dominated by a narrow and intense throughflow as part of the Caribbean Current. The intense throughflow enters

the northwestern Caribbean Sea along the outer flank of Nicaragua Rise and then flows westward about 200 to 300 km off the northern coast of Honduras. The throughflow veers anticyclonically to flow northward along the eastern coast of Belize and Mexico after passing the Gulf of Honduras. The simulated sub-surface temperature at day 720 produced by the SSP2W nested inner model is characterized by a narrow strip of relatively warm water that is advected by the Caribbean Current from the outer flank of Nicaragua Rise to the western part of Cayman and Yucatan Basins. Figure 8b also demonstrates several pools of relatively cold sub-surface water associated with local upwelling near the northern coast of Honduras and east coast of Yucatan Peninsula.

The SSP2W nested inner model generates more intense throughflow over the northwestern Caribbean with more meso-scale features (Fig. 8b) than the SSP2W nested outer model (Fig. 8a), due to the finer horizontal resolution used in the inner model. The inner model results in the SSP1W case compare very well to those in the SSP2W case (Fig. 8b,c), indicating that the feedback from the inner model to the outer model plays a secondary role in affecting the inner model results. In comparison, the inner model results in the OSP2W and OSP1W cases (Fig. 8d,e) have large-scale features consistent with those in the SSP2W and SSP1W cases, but with much less meso-scale features in the former two cases due to the smoothing effect of the the original semi-prognostic method discussed in section 2. Of particular note, are the much more pronounced cold pools near the northern coast of Honduras in the SSP compared to the OSP cases.

In comparison with the model results shown in Fig. 8b-e, the sub-surface circulation at day 920 produced by the inner model in the C1W case (Fig. 8f) differs significantly from the inner model results using the four variants of the new nesting technique. The simulated sub-surface throughflow over the northwest Caribbean Sea produced by the C1W nested inner model is too close the north coast of Honduras. The large-scale anticyclonic gyre over the western Yucatan Basin produced by the C1W nested inner model also differs significantly from the inner model results in other four cases.

We also calculate the annual mean near-surface currents at 16 m from the second year inner model simulation (Fig. 9) and compare them with Fratantoni's decadal mean

near-surface currents in the northwestern Caribbean Sea. The time-mean near-surface currents produced by the inner model in the SSP2W, SSP1W and OSP2W and OSP1W cases (Fig. 8b-e) are characterized by a persistent throughflow that enters the Cayman Basin from the outer flank of Nicaragua Rise to form a narrow westward flow off the northern coast of Honduras. This westward jet turns anticyclonically to run northward along the eastern coast of Belize and Mexico after passing the Gulf of Honduras, and compares well with the observed near-surface currents in the region. The γ^2 values are about 0.35 for the inner model results in the SSP2W and SSP1W cases and 0.36 in the OSP2W and OPS1W cases (Table 1 and Fig. 10b-c). Therefore, the all the four types of the new nesting technique perform equally well in reproducing Fratantoni's time-mean near-surface currents in the northwest Caribbean Sea.

The time-mean sub-surface circulation produced by the C1W nested inner model (Fig. 9f) has large-scale features compare qualitatively to the observed currents, with the simulated throughflow spreading too much to the Gulf of Honduras and deep water of the central Yucatan Basin. The γ^2 value in the C1W case is about 0.39 (Fig. 10f), which is lightly larger than the values in other four cases. The outer model in the SSP2W case fits the data the least well (Fig. 9a and 10a) with Fratantoni's data, with the γ^2 value of about 0.43. Due mainly to the coarse resolution, the outer model underestimates the observed currents significantly, with the simulated throughflow too broad in comparison with the inner model results in other four cases.

5. Summary and conclusion

A new two-way nesting technique based on the smoothed semi-prognostic (SSP) method (Eden et al. 2004) has been developed for a nested-grid ocean circulation modelling system. The SSP method is a modification of the original semi-prognostic (OSP) method introduced by Sheng et al. (2001). The original application of both the SSP and OSP methods was to adjust a model to correct for systematic error in multi-year simulations (see Greatbatch et al. 2004 for a comprehensive review). In this paper, we have demonstrated that both the SSP and OSP methods can be used to exchange information between the sub-components of a nested-grid modelling system

by introducing an interaction term in the model horizontal momentum equations. The new nesting technique is very easy and straightforward to implement in the model code since only the hydrostatic equations in the subcomponents of the nested-grid modelling system need to be modified. The new nesting technique can also easily be applied to a multiple nested-grid modelling system; that is a system with several fine-resolution inner models embedded inside a coarse-grid outer model, and one or more finer-resolution local models embedded inside each inner model. The main advantage of semi-prognostic nesting is that because the outer model is used to constrain the inner model within the interior of the inner model domain, unrealistic drift of the inner model is effectively prevented.

Depending on the use of the SSP or OSP methods and one-way or two-way nesting, four different types of the new nesting technique were introduced in this paper. They are the SSP two-way (SSP2W), SSP one-way (SSP1W), OSP two-way (OSP2W), and OSP one-way (OSP1W) nesting techniques. The common features of these four types of the new technique are that (1) the inner model open boundary conditions are specified based on the outer model results; and (2) the outer model results are used to constrain the inner model momentum equations over the interior of the inner model domain based on the semi-prognostic method. The main difference between the SSP and OSP nesting techniques is that the SSP nesting technique uses a spatially smoothed (large-scale) interaction term, while the OSP nesting technique uses an unsmoothed interaction term. Smoothing of the interaction term in the SSP case releases the fine scales associated with the inner model grid, ensuring that the maximum benefit is obtained from the higher resolution of the inner model, while at the same time still using the outer model to constrain the inner model on large spatial scales (large compared to the smoothing scale). The main difference between the one-way and two-way nesting using the SSP or OSP method is that the inner model density is used to adjust the outer model hydrostatic equation over the overlapping subregion in two-way nesting, while there is no feedback from the inner model to the outer model in the one-way nesting. In comparison, the conventional one-way (C1W) nesting technique connects the inner model to the outer model only through the specification of the inner model boundary

conditions taken from the outer model. The C1W nesting technique does not allow the outer model to constrain directly the inner model results over the interior of the inner model domain, neither does it allow any feedback from the inner model to the outer model.

The performance of the four versions of the new nesting technique, as well as C1W nesting, was assessed using two independent nested-grid ocean circulation modelling systems, with one for the Meso-American Barrier Reef System (MBRS) northwest Caribbean Sea and the other for the Scotian Shelf of the northwest Atlantic Ocean. Both nested systems comprise a fine-resolution inner model and a coarse-resolution outer model. Comparison of the instantaneous circulation and temperature field produced by the inner models demonstrates that the SSP2W nesting technique performs better than the SSP1W, OSP2W and OSP1W nesting techniques and much better than the C1W nesting technique. We also assessed the performance of the new nesting technique by comparing the annual mean near-surface currents produced by the five different nesting methods with the decadal-mean near-surface currents estimated by Fratantoni (2001) from the observed trajectories of sub-surface drifters in the 1990s. We found that the SSP2W and SSP1W nesting techniques perform equally well and both methods perform significantly better than the C1W nesting technique in reproducing time-mean near-surface circulation in the MBRS of the northwestern Caribbean Sea and Scotian Shelf of the northwestern Atlantic Ocean. This indicates the importance of adjusting the interior of the inner model using outer model fields (a feature of semi-prognostic nesting), while the feedback from the inner model to the outer model plays a less important role in affecting the annual mean circulation in the two study regions.

Acknowledgments

We wish to thank Carsten Eden for his initial suggestion of developing a two-way nesting technique based on the smoothed semi-prognostic method. We also thank Chris Mooers, Alan Davies, Jiuxing Xing and Leo Oey for their useful comments. We thank David Fratantoni for providing the near-surface currents determined from the 10 m-drogued satellite-tracked drifters in the North Atlantic. This work has been supported by funding from CFCAS and NSERC. R.J.G. and J.S. are also supported by NSERC,

MARTEC (a Halifax based company), and the Meteorological Service of Canada (MSC) through the NSERC/MARTEC/MSC Industrial Research Chair in "Regional Ocean Modelling and Prediction".

References

Barnier B, Siefridt L, Marchesiello P (1995) Thermal forcing for a global ocean circulation model using a three-year climatology for ECMWF analyses. J Marine Systems 6: 363-380

Bell MJ, Martin MJ, Nichols NK (2004) Assimilation of data into an ocean model with systematic errors near the equator. Q J R Meterol Soc 130: 873-893

Csanady GT (1982) Circulation in the Coastal Ocean. New York, 279 pp

Eden C, Greatbatch RJ, Böning CW (2004) Adiabatically correcting an eddy-permitting model of the North Atlantic using large-scale hydrographic data. J Phys Oceanogr 34: 701-719

Dengg J, Boening CW, Ernst U, Redler R, Beckmann A (1999) Effects of an improved model representation of overflow water on the subpolar North Atlantic. International WOCE Newsletter 37: 10-15

Fox AD, Maskell SJ (1995) Two-way interactive nesting of primitive equation ocean models with topography. J Phys Oceanogr 25: 2977-2996

Fratantoni DF (2001) North Atlantic surface circulation during the 1990's observed with satellite-tracked drifters. J Geophys Res 106: 22067-22093

Geshelin Y, Sheng J, Greatbatch RJ (1999) Monthly mean climatologies of temperature and salinity in the western North Atlantic. Can Data Rep Hydrogr Ocean Sci 153: 62 pp

Ginis I, Richardson A, Rothstein L (1998) Design of a multiply nested primitive equation ocean model. Mon Wea Rev 126: 1054-1079

Greatbatch RJ, Fanning AF, Goulding AD, Levitus S (1991) A diagnosis of interpentadal circulation changes in the North Atlantic. J Geophys Res 96: 22009-22023

Greatbatch RJ, Sheng J, Eden C, Tang L, Zhai X, Zhao J (2004) The semi-prognostic method. Continental Shelf Res (in press)

Kurihara Y, Tripoli GJ, Bender MA (1979) Design of a movable nested-mesh primitive equation model. Mon Wea Rev 107: 239-249

Johns WE, Townsend TL, Fratantoni DM, Wilson WD (2002) On the Atlantic inflow to the Caribbean Sea. Deep-Sea Res I 49: 211-243

Large WG, McWilliams JC, Doney, SC (1994) Oceanic vertical mixing: A review and a model with a nonlocal boundary layer parameterization. Reviews of Geophysics 32: 363-403

Lazier JRN, Wright DG (1993) Annual velocity variations in the Labrador Current. J Phys Oceanogr 23: 659-679

Loder J, Petrie B, Gawarkiewicz G (1998) The coastal ocean off northestern north America: a large-scale view. The Sea 11: 105-133

Marchesiello P, McWilliams JC, Shchepetkin A (2001) Open boundary conditions for long-term integration of regional oceanic models. Ocean Modelling 3: 1-20

Mooers CNK, Maul GA (1998) Intra-Americas Sea circulation, coastal segment(3,W). The Sea 11: John Wiley and Sons 183-208

Oey LY, Chen P (1992) A nested-grid ocean model: with application to the simulation of meanders and eddies in the Norwegian Coastal Current. J Geophys Res 97: 20063-20086

Orlanski I (1976) A simple boundary condition for unbounded hyperbolic flow. J Comput Phys 21: 251-269

Sheng J, Tang L (2003) A numerical study of circulation in the western Caribbean Sea. J Phys Oceanogr 33: 2049-2069

Sheng J, Tang L (2004) A two-way nested-grid ocean circulation model for the Meso-American Barrier Reef System. Ocean Dynamics 54: 10.1007/s10236-003-0074-3 232-242

Sheng J, Thompson KR (1996) A robust method for diagnosing regional shelf circulation from scattered density profiles. J Geophys Res 101: 25647-25659

Sheng J, Greatbatch RJ, Wright DG (2001) Improving the utility of ocean circulation models through adjustment of the momentum balance. J Geophys Res 106: 16711-16728

Sheng J, Zhai X, Greatbatch RJ (2004) Numerical study of the storm-induced circulation on the Scotian Shelf during Hurricane Juan using a nested-grid ocean model. Prog Oceangr: (in prep)

Sheng J, Wright DG, Greatbatch RJ, Dietrich D (1998) CANDIE: a new version of the DieCAST ocean circulation Model. J Atm and Oceanic Tech 15: 1414-1432

Smagorinsky J (1963) General circulation experiments with the primitive equation. I. The basic experiment. Monthly Weather Review 21: 99-165

Smith PC, Petrie B, Mann CR (1978) Circulation, variability and dynamics of the Scotian Shelf and Slope. J Fish Res Board Can 35: 1067-1083

Zhai X, Sheng J, Greatbatch RJ (2004) A New Two-Way Nested-Grid Ocean Modelling Technique Applied to the Scotian Shelf and Slope. Estuarine and coastal modeling: Proceedings of the 8th international conference, in press

Zhao J, Greatbatch RJ, Sheng J, Eden C, Azetsu-Scott K (2004) Improvement in the transport of CFCs in a model of the North Atlantic that uses an adiabatical correction technique. schemes. G Res Lett 31: 10.1029/2005GL020206, L12309

Received ; revised ; accepted .

Table 1. Specifications of the four versions of the new nesting technique based on the smoothed semi-prognostic method and the conventional one-way nesting technique, and the γ^2 values used to assess the performance of these techniques using two independent nested-grid systems, one for the Scotian Shelf (SS) and the other for the Meso-American Barrier Reef System (MBRS).

			Nesting coefficients		γ^2 value	
Index	Technique	Correction Term	β_i	β_o	SS	MBRS
1	SSP2W	Smoothed	0.5	0.5	0.61	0.35
2	SSP1W	Smoothed	0.5	1.0	0.61	0.35
3	OSP2W	Unmoothed	0.5	0.5	0.65	0.36
4	OSP1W	Unmoothed	0.5	1.0	0.65	0.36
5	C1W		1.0	1.0	1.01	0.39

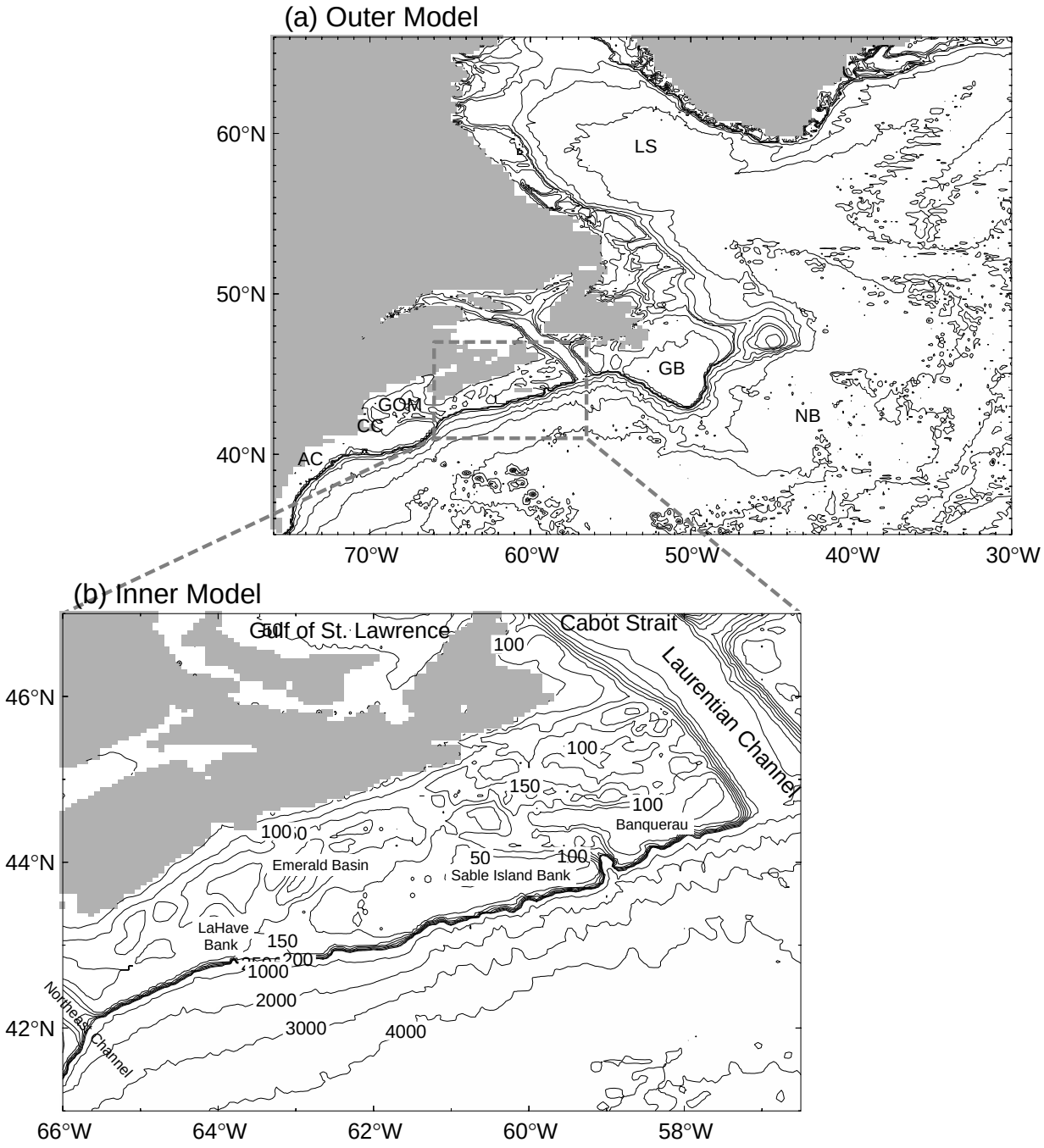

Figure 1: Bathymetric features within (a) the outer model domain of the northwest Atlantic Ocean, and (b) the inner model domain of the Scotian Shelf and slope. Abbreviations are used for the Labrador Sea (LS), Newfoundland Basin (NB), Grand Banks (GB), Gulf of Maine (GOM), Cape Cod (CC) and Atlantic City (AC).

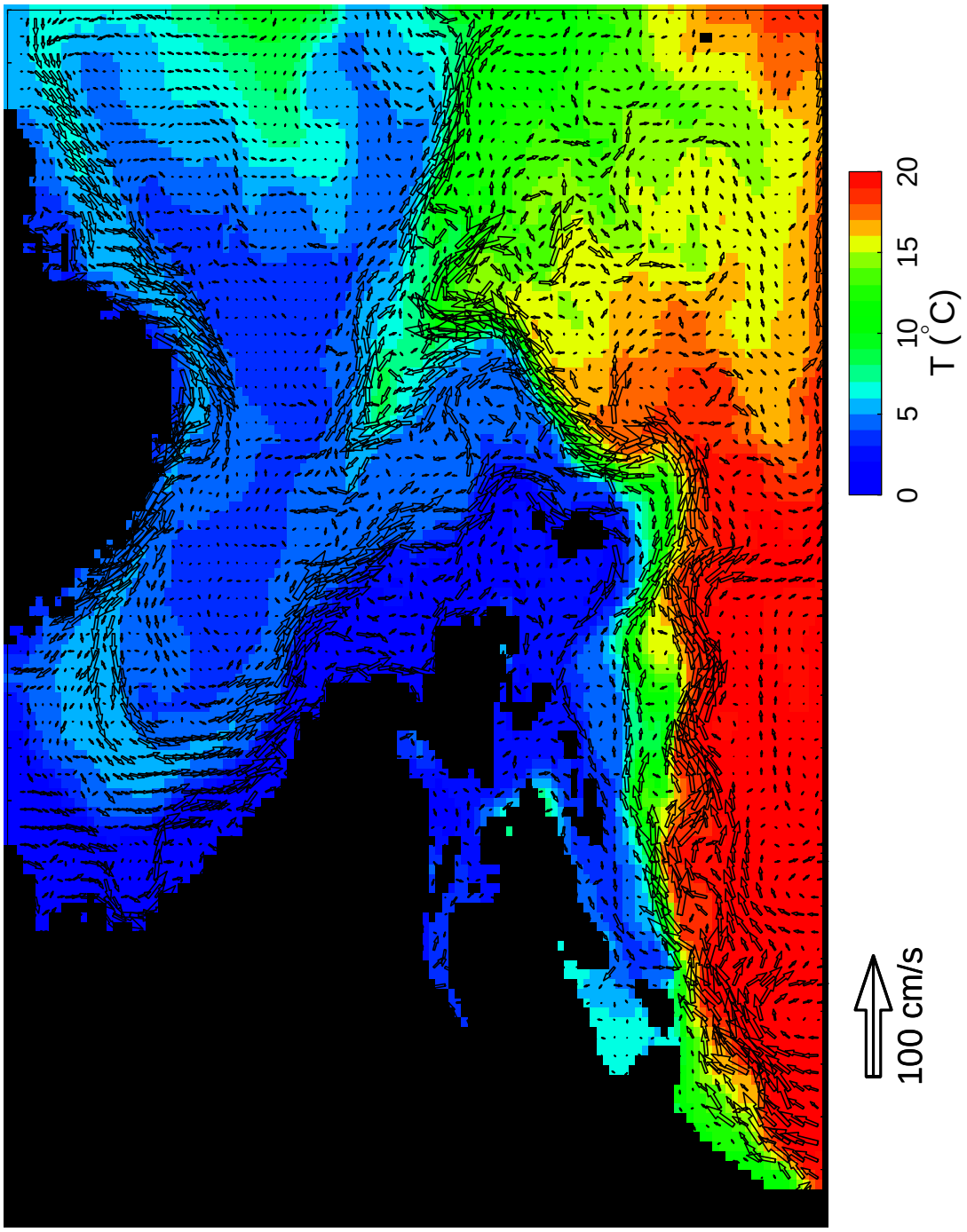

Figure 2: Sub-surface (61 m) temperature and currents (arrows) at day 690 over the northwest Atlantic Ocean produced by the outer model in the SSP2W case. Velocity vectors are plotted at every second model grid point.

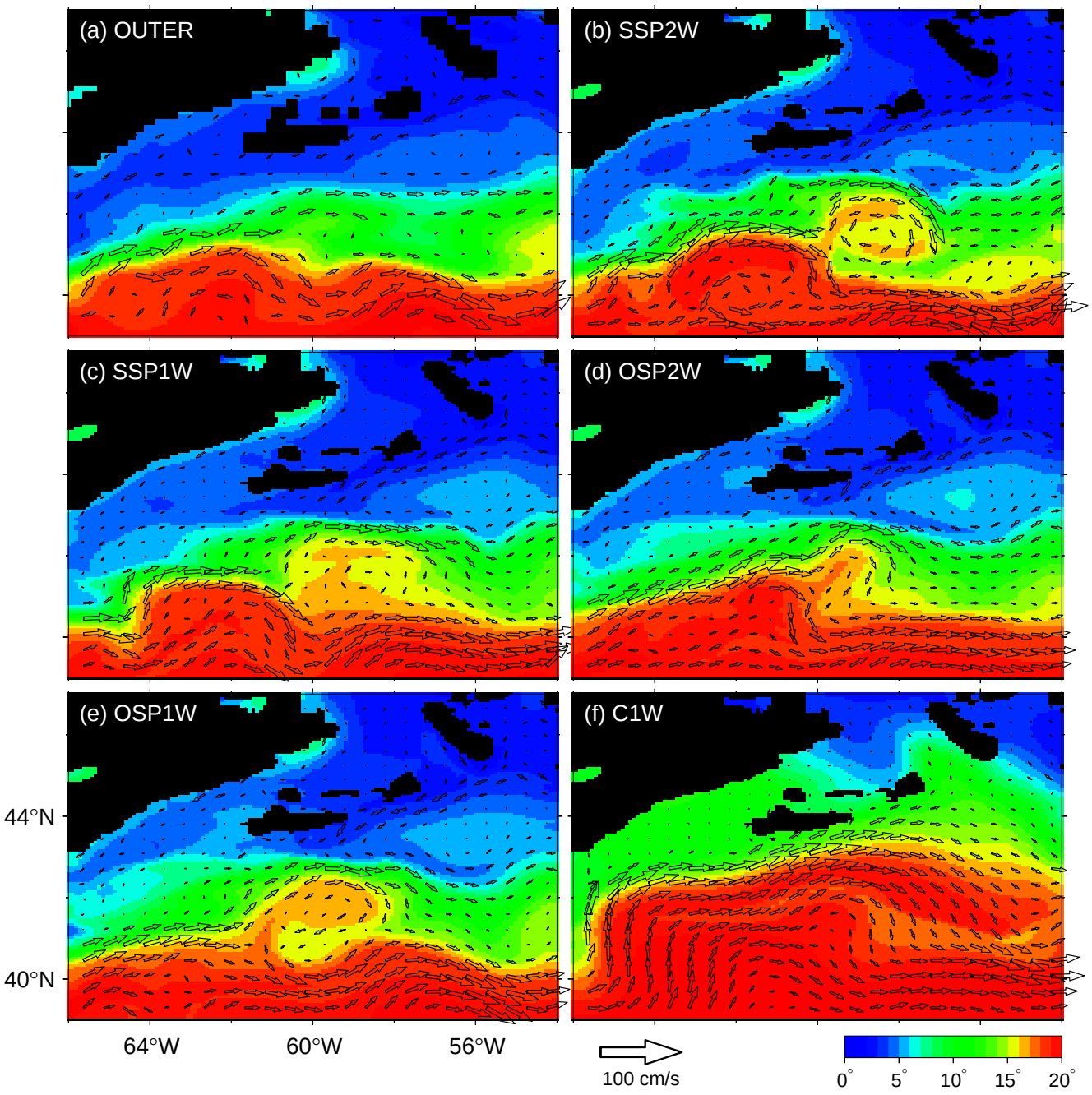

Figure 3: Simulated sub-surface (61 m) temperature and currents (arrows) at day 690 over the Scotian Shelf and slope produced by (a) the outer model using the SSP2W nesting technique and the inner model using (b) the SSP2W, (c) SSP1W, (d) OSP2W, (e) OSP1W, and (f) C1W nesting techniques. Velocity vectors are plotted at every fourth model grid point for the inner model and every second model grid point for the outer model over the inner model domain.

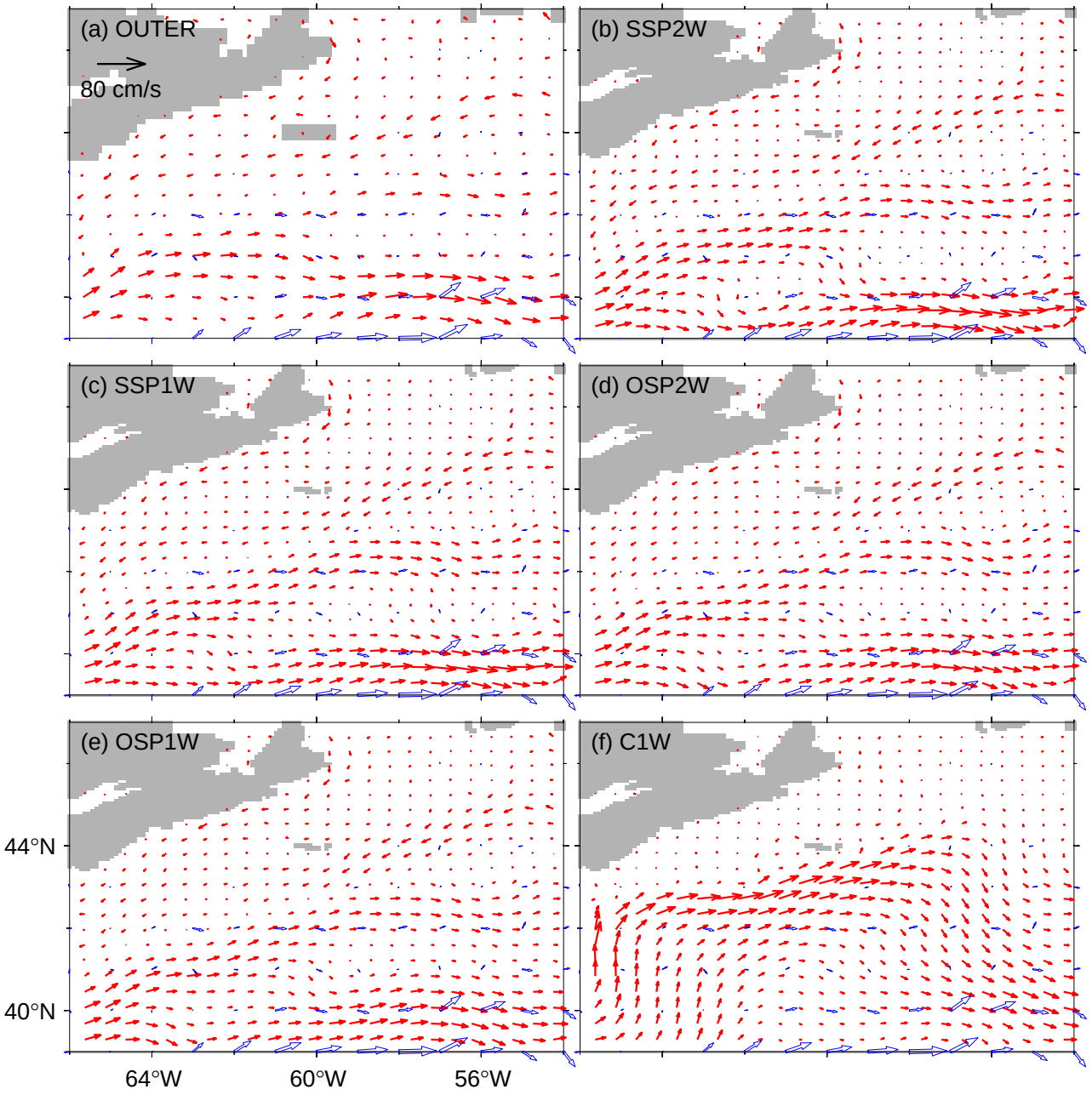

Figure 4: Comparison of simulated (solid red arrows) and observed (open black arrows) near-surface currents over the Scotian Shelf and slope. The observed currents are the gridded time-mean near-surface currents during the 1990s inferred from trajectories of 15 m-drogued satellite-tracked drifters by Fratantoni (2001) on a 1° grid. The simulated currents are the annual mean currents at 16 m calculated from the second year model results generated by (a) the outer model using the SSP2W nesting technique and those by the inner model using (b) the SSP2W, (c) SSP1W, (d) OSP2W, (e) OSP1W, and (f) C1W nesting techniques. Velocity vectors are plotted at every fourth model grid point for the inner model and every second model grid point for the outer model.

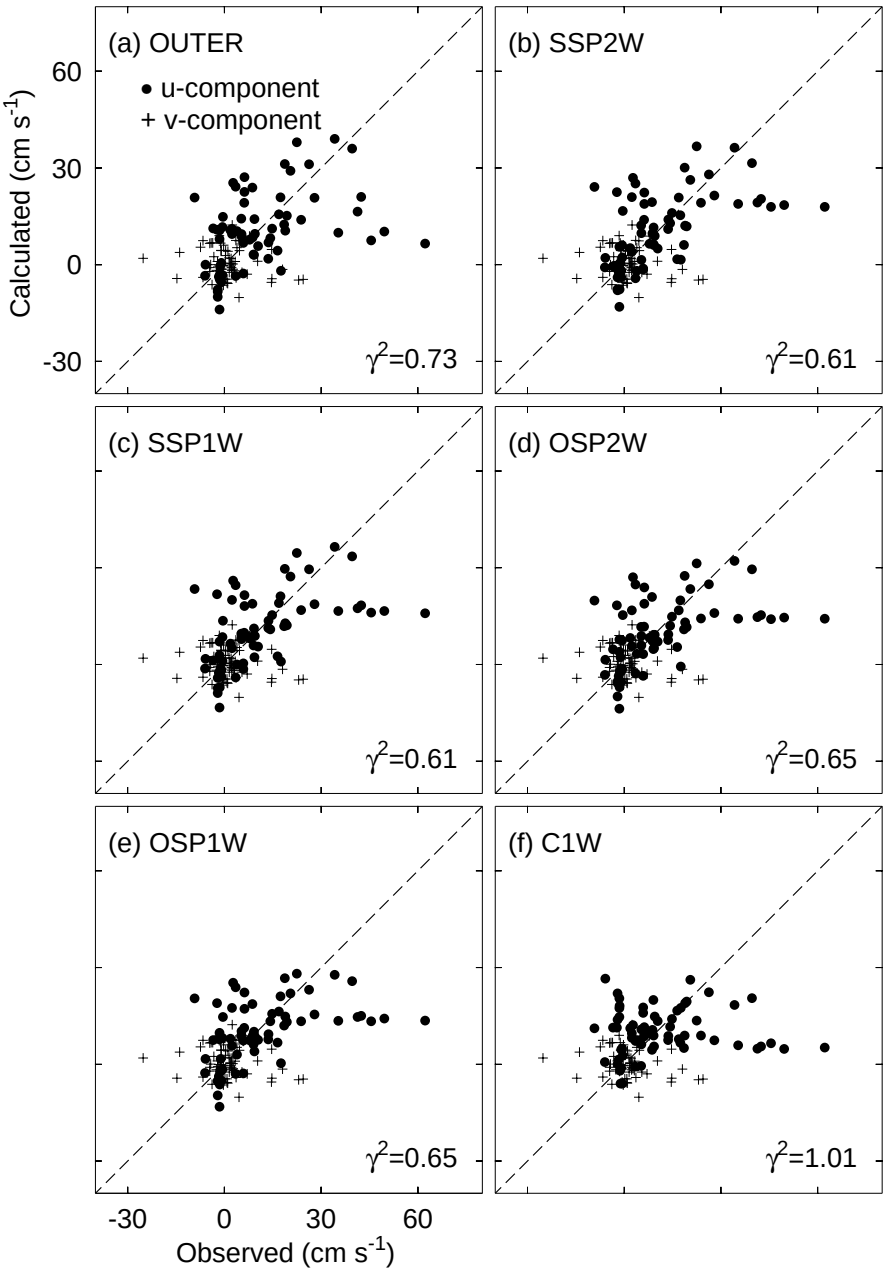

Figure 5: Scatterplots of observed and simulated time-mean near-surface currents over the Scotian Shelf and slope. The observed currents are the decadal-mean near-surface currents during the 1990s inferred from trajectories of 15 m-drogued satellite-tracked drifters (Fratantoni, 2001). The simulated time-mean currents are those at the same locations as the observations interpolated from the annual mean circulation calculated from the second year model simulations at 16 m produced by (a) the outer model using the SSP2W nesting technique by the inner model using (b) the SSP2W, (c) SSP1W, (d) OSP2W, (e) OSP1W, and (f) C1W nesting techniques. Dashed line represents perfect fit for reference.

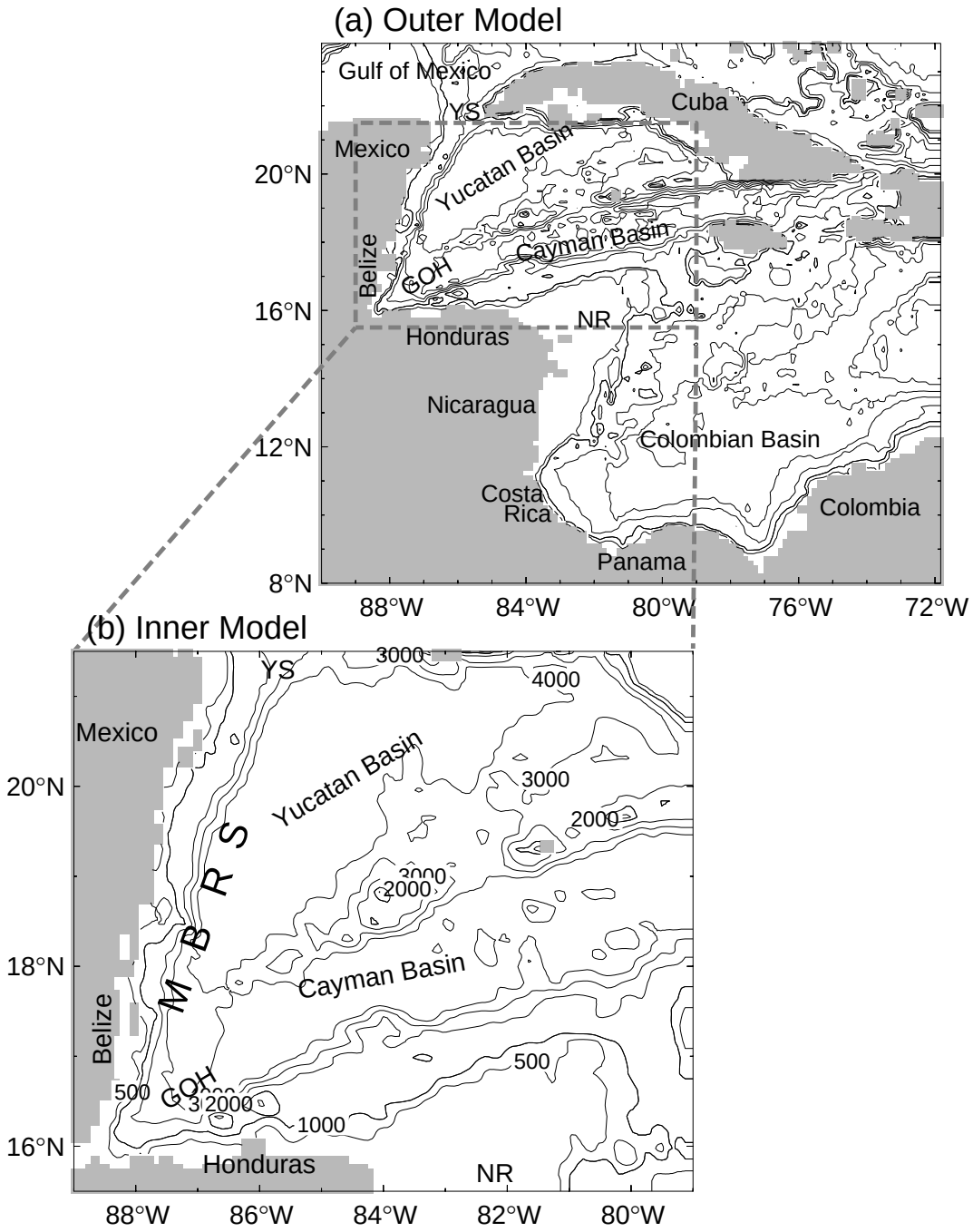

Figure 6: Bathymetric features within (a) the outer model domain of the western Caribbean Sea, and (b) the inner model domain of the Meso-American Barrier Reef System. Abbreviations are used for Yucatan Strait (YS), Gulf of Honduras (GOH) and Nicaragua Rise (NR).

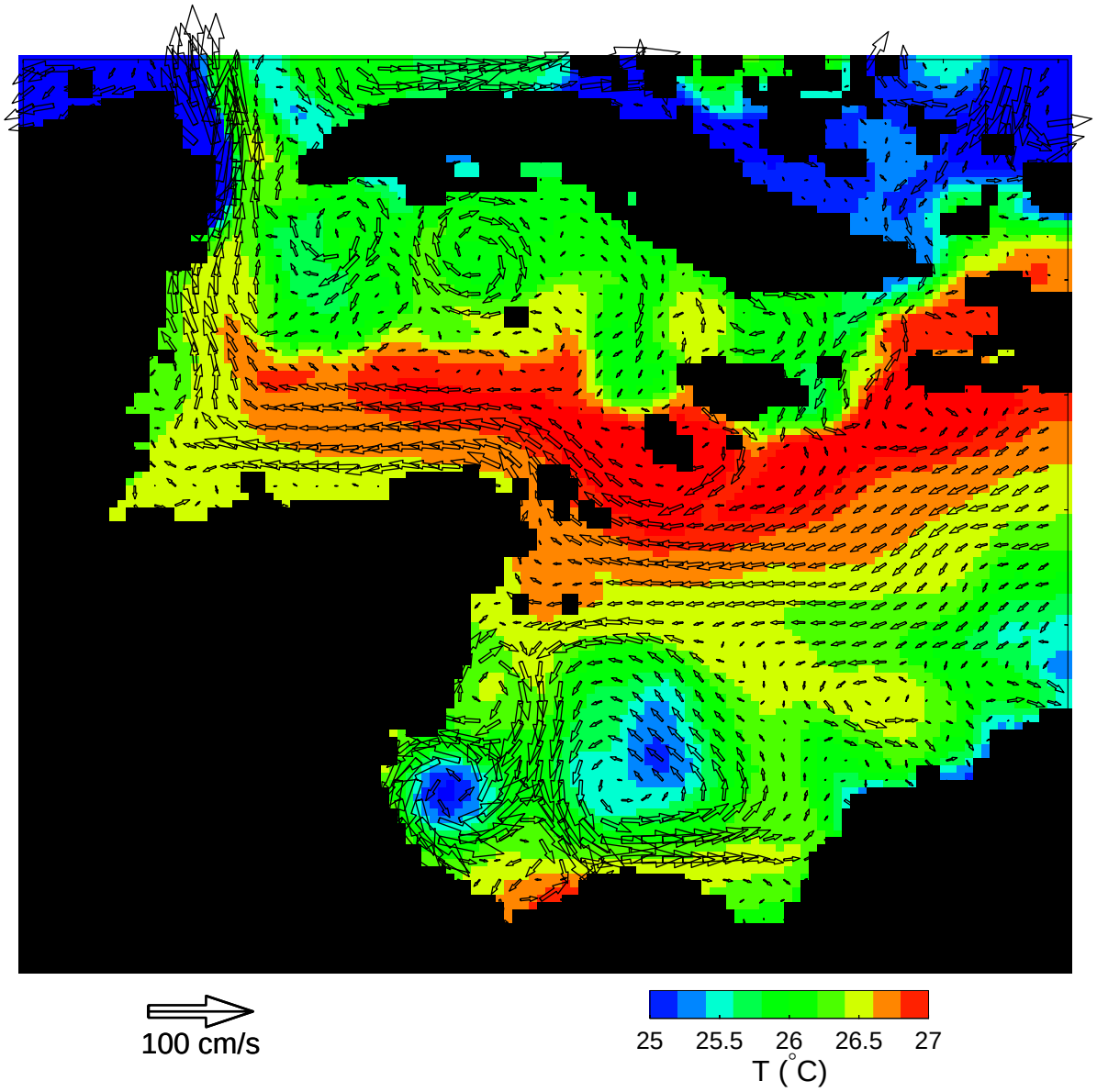

Figure 7: Simulated sub-surface (61 m) temperature and currents (arrows) at day 720 over the western Caribbean Sea produced by the SSP2W nested outer model. Velocity vectors are plotted at every second model grid point.

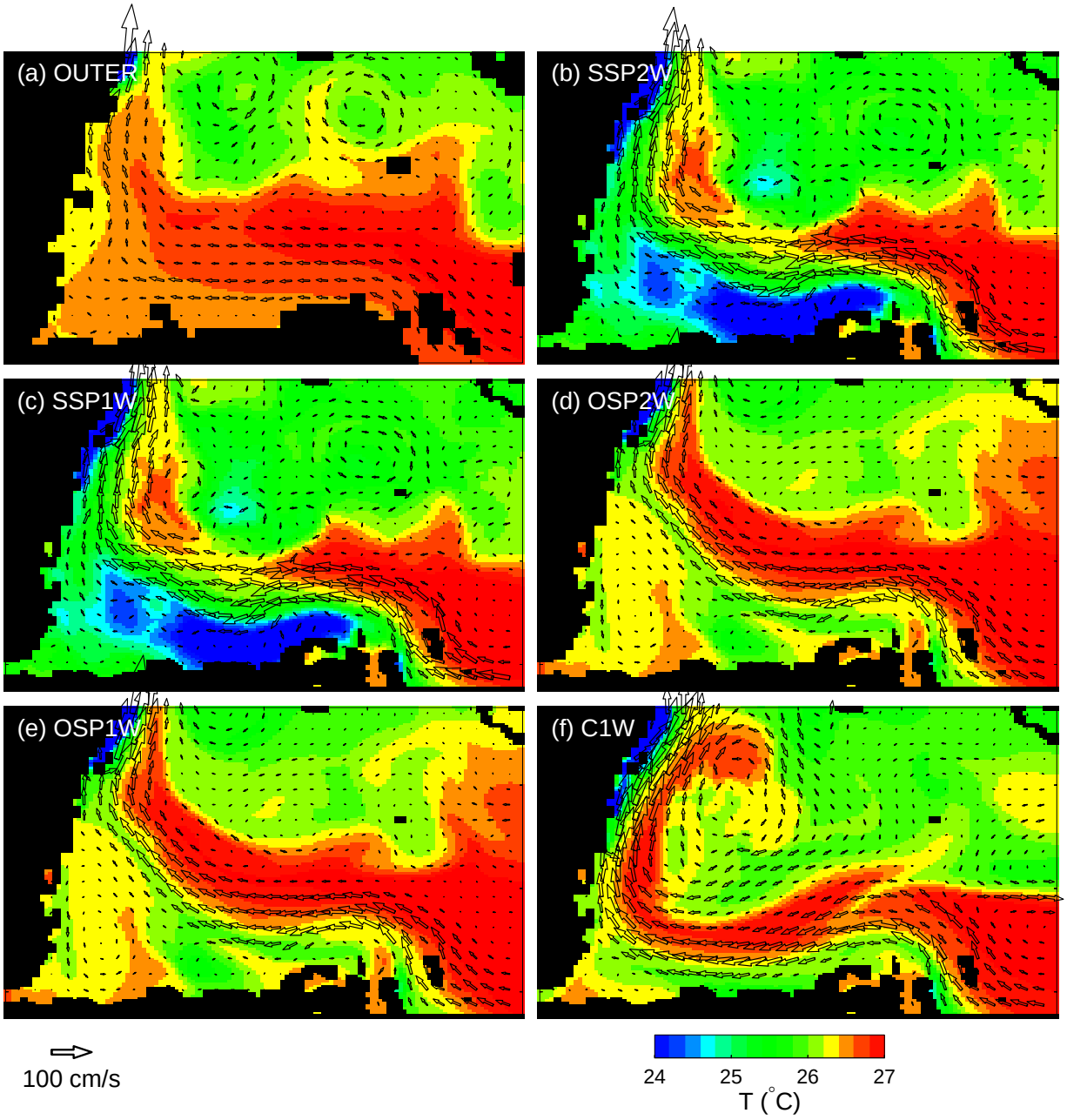

Figure 8: Simulated sub-surface (61 m) temperature and currents (arrows) at day 720 over the northwest Caribbean Sea produced by the outer model using the SSP2W nesting technique and those by the inner model using (b) the SSP2W, (c) SSP1W, (d) OSP2W, (e) OSP1W, and (f) C1W nesting techniques. Velocity vectors are plotted at every fifth model grid point for the inner model and every second model grid point for the outer model.

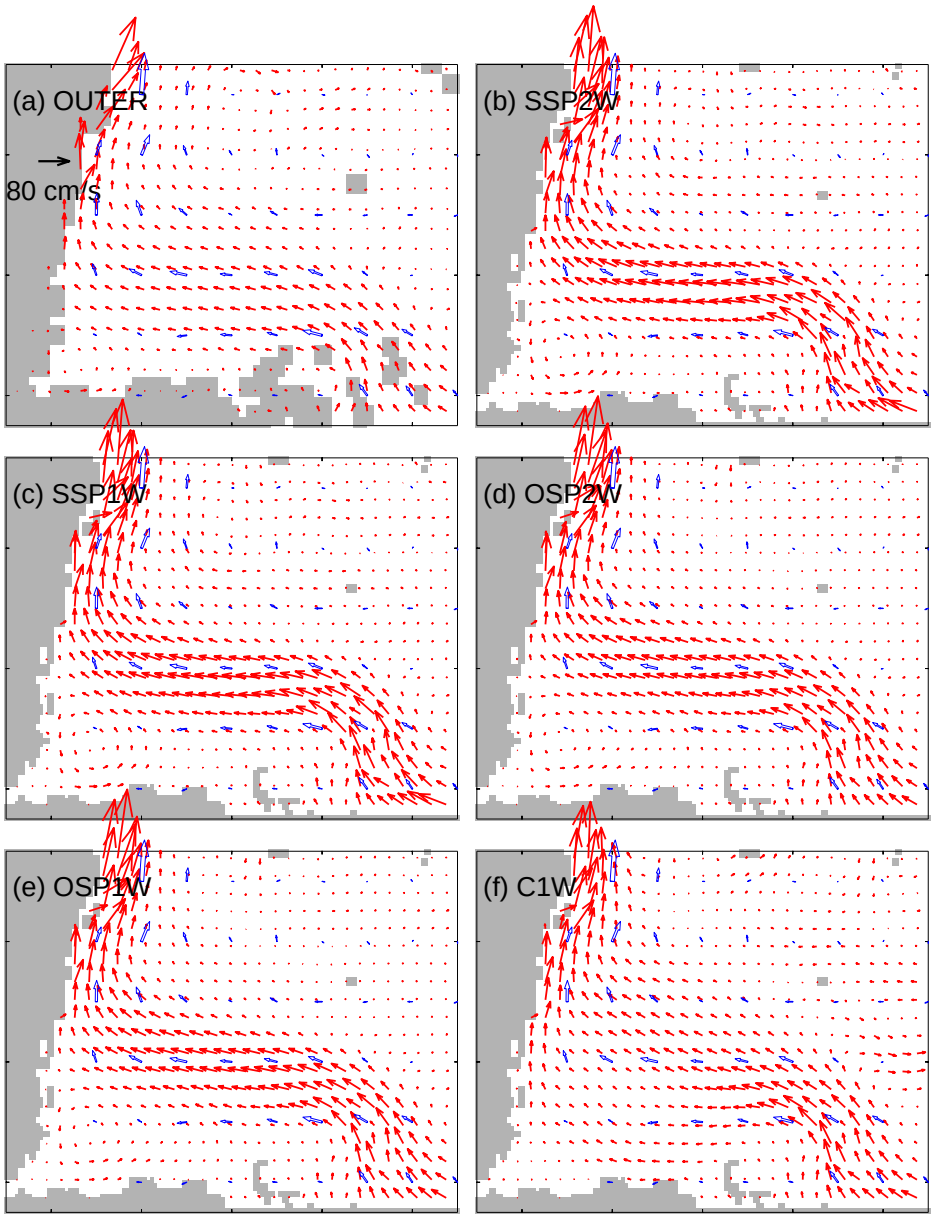

Figure 9: Comparison of simulated (solid arrows) and observed (open arrows) near-surface currents over the northwestern Caribbean Sea. The observed currents are the gridded time-mean near-surface currents during the 1990s inferred from trajectories of 15 m-drogued satellite-tracked drifters by Fratantoni (2001) on a 1° grid. The modeled currents are the annual mean currents at 16 m computed from the second year model results generated by the outer model using the SSP2W nesting technique and those by the inner model using (b) the SSP2W, (c) SSP1W, (d) OSP2W, (e) OSP1W, and (f) C1W nesting techniques. Velocity vectors are plotted at every fifth model grid point for the inner model and every second model grid point for the outer model.

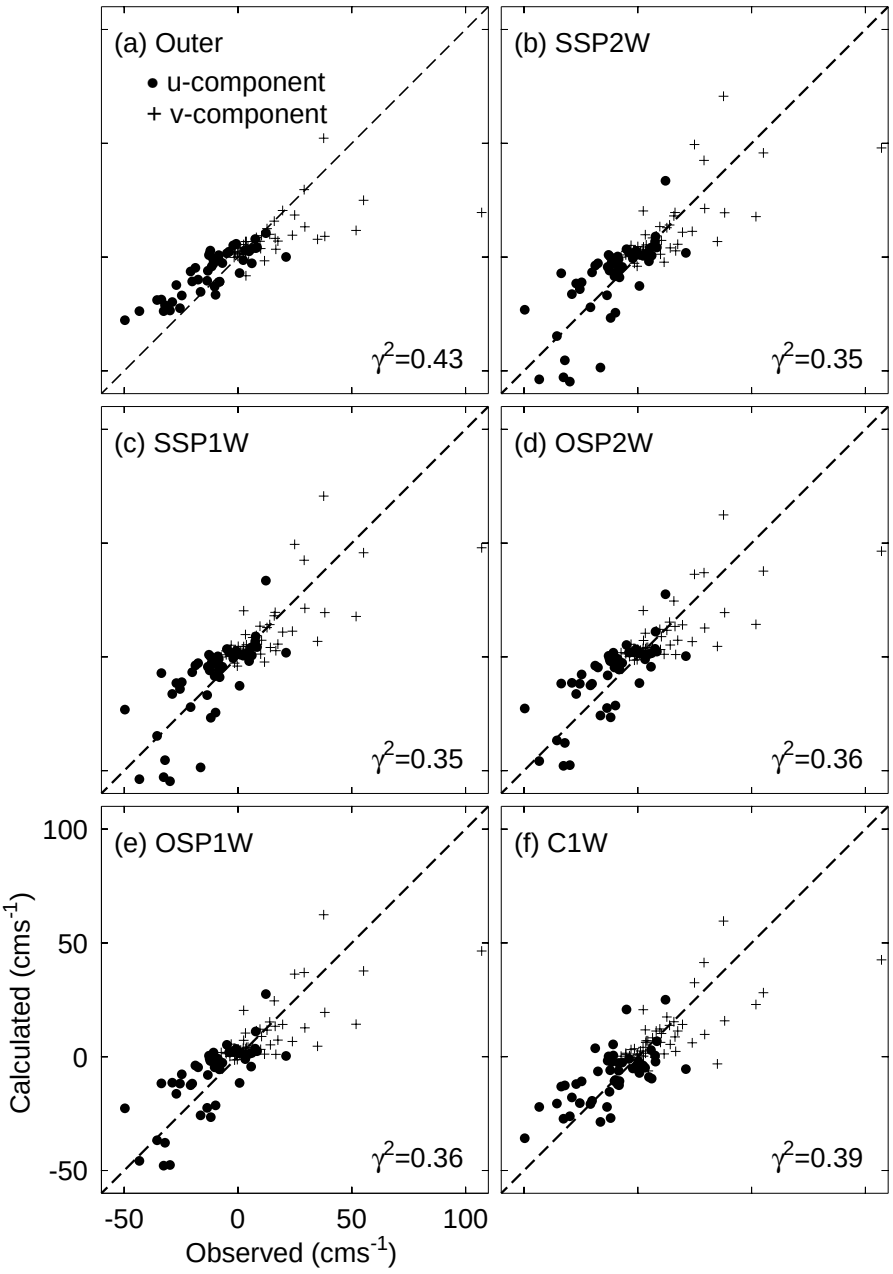

Figure 10: Scatterplots of observed and model-computed time-mean near-surface currents in the northwest Caribbean Sea. The observed currents are the decadal-mean near-surface currents during the 1990s inferred from trajectories of 15 m-drogued satellite-tracked drifters by Fratantoni (2001). The model-computed currents are those at the same locations as the observations interpolated from the second year model simulations at 16 m by the outer model using the SSP2W nesting technique and those by the inner model using (b) the SSP2W, (c) SSP1W, (d) OSP2W, (e) OSP1W, and (f) C1W nesting techniques. Dashed line represents perfect fit for reference.